

Anomalous Hall effect from nonlinear magnetoelectric coupling

Longju Yu,¹ Hong Jian Zhao,^{1,2,3,4} Yurong Yang,^{5,6} Laurent Bellaiche,^{7,8} and Yanming Ma^{1,3,4}

¹Key Laboratory of Material Simulation Methods and Software of Ministry of Education,
College of Physics, Jilin University, Changchun 130012, China

²Key Laboratory of Physics and Technology for Advanced Batteries (Ministry of Education),
College of Physics, Jilin University, Changchun 130012, China

³State Key Laboratory of Superhard Materials, College of Physics, Jilin University, Changchun 130012, China

⁴International Center of Future Science, Jilin University, Changchun 130012, China

⁵National Laboratory of Solid State Microstructures, Nanjing University, Nanjing 210093, China

⁶Jiangsu Key Laboratory of Artificial Functional Materials,
Department of Materials Science and Engineering, Nanjing University, Nanjing 210093, China

⁷Smart Ferroic Materials Center, Physics Department and Institute for Nanoscience and Engineering,
University of Arkansas, Fayetteville, Arkansas 72701, USA

⁸Department of Materials Science and Engineering,
Tel Aviv University, Ramat Aviv, Tel Aviv 6997801, Israel

The anomalous Hall effect (AHE) is a topology-related transport phenomenon being of potential interest in spintronics, because this effect enables the efficient probe of magnetic orders (i.e., data readout in memory devices). It is well known that AHE spontaneously occurs in ferromagnets or antiferromagnets with magnetization. While recent studies reveal electric-field induced AHE (via linear magnetoelectric coupling), an AHE originating from *nonlinear* magnetoelectric coupling remains largely unexplored. Here, by symmetry analysis, we establish the phenomenological theory regarding the spontaneous and electric-field driven AHE in magnets. We show that a large variety of magnetic point groups host an AHE that is driven by uni-axial, bi-axial, or tri-axial electric field and that comes from nonlinear magnetoelectric coupling. Such electric-field driven anomalous Hall conductivities are reversible by reversing the magnetic orders. Furthermore, our first-principles calculations suggest Cr₂O₃ and CoF₂ as candidates hosting the aforementioned AHE. Our work emphasizes the important role of nonlinear magnetoelectric coupling in creating exotic transport phenomena, and offers alternative avenues for the probe of magnetic orders.

Introduction.— The anomalous Hall effect (AHE) is a fundamental transport phenomenon where an applied voltage induces an transverse Hall current response [1–18]. Nowadays, the AHE not only becomes an important platform for exploring topology-related transport properties [1–5], but also offers an efficient way to probe magnetic order — being of potential value in spintronics [18–21]. The AHE was found to spontaneously occur in ferromagnets [1–3, 5–9] or antiferromagnets with specific magnetic configurations [10–18]. As a matter of fact, antiferromagnetic materials with symmetry-allowed weak or tiny magnetization likewise enable AHE [13, 22, 23]. By this, it is anticipated that external fields capable of inducing magnetization should, in principle, induce AHE as well. In this regard, magnetoelectric coupling (linear or nonlinear effect) [24–26] are interesting avenues for electric-field driven AHE. Indeed, recent studies demonstrate that gate voltage can induce AHE via linear magnetoelectric coupling (e.g., the layer Hall effect and electric Hall effect [27–31]); Yet, the electric-field induced AHE arising from nonlinear magnetoelectric coupling remains largely unexplored.

Here, we use group-theoretical approach to establish the phenomenological theory for spontaneous and electric-field driven AHE in crystalline materials. Our symmetry analysis demonstrates that both type-I and type-III magnetic point groups (MPGs) [32] exhibit spontaneous AHE or electric-field induced AHE from

linear or nonlinear magnetoelectric coupling. We highlight that nonlinear magnetoelectric AHE is accommodated by a wide spectrum of MPGs, where the anomalous Hall conductivity component is (i) achieved by applying uni-axial, bi-axial, or tri-axial electric field and (ii) reversible by reversing the magnetic orders. Following our theory and confirmed by first-principles calculations, we further suggest that Cr₂O₃ and CoF₂ are representative materials towards the electric-field induced AHE via nonlinear magnetoelectric coupling.

Anomalous Hall effect and Hall vector. — The AHE is characterized by $J_\alpha = \sum_\beta \sigma_{\alpha\beta} E_\beta$, with $\sigma_{\alpha\beta}$ being the transverse conductivity (i.e., $\alpha \neq \beta$), E_β the electric field along β direction, and J_α the current density along α direction. Generally, the anomalous Hall conductivity $\sigma_{\alpha\beta}$ stems from intrinsic [2, 3, 6, 10–14] and extrinsic mechanisms [7–9]. This work focuses on the intrinsic mechanism. According to Refs. [5, 15], the $\sigma_{\alpha\beta}$ conductivity is expressed as

$$\sigma_{\alpha\beta} = - \sum_{n\gamma} \epsilon_{\alpha\beta\gamma} \frac{e^2}{\hbar} \int \frac{d\mathbf{k}}{(2\pi)^3} f(\epsilon_{n\mathbf{k}}) \Omega_{\gamma,n\mathbf{k}}, \quad (1)$$

where $\epsilon_{\alpha\beta\gamma}$ is the Levi-Civita symbol ($\alpha, \beta, \gamma = x, y, z$), e the charge of the electron, \hbar the reduced Planck constant, $\epsilon_{n\mathbf{k}}$ energy eigenvalue, $f(\epsilon_{n\mathbf{k}})$ the Fermi-Dirac distribution function, and $\Omega_{\gamma,n\mathbf{k}}$ the Berry curvature (n

being the band index, \mathbf{k} being the wave vector). In Eq. (1), the Levi-Civita symbol $\epsilon_{\alpha\beta\gamma}$ implies the anti-symmetric nature of the anomalous Hall conductivity, that is, $\sigma_{\alpha\beta} = -\sigma_{\beta\alpha}$. This enables the definition of a Hall vector $\mathcal{M} \equiv (\mathcal{M}_x, \mathcal{M}_y, \mathcal{M}_z) \equiv (\sigma_{zy}, \sigma_{xz}, \sigma_{yx})$, a current density vector $\mathbf{J} \equiv (J_x, J_y, J_z)$ and an electric field vector $\mathbf{E} \equiv (E_x, E_y, E_z)$ so that the AHE is described by $\mathbf{J} = \mathcal{M} \times \mathbf{E}$ [13, 15]. From symmetry point of view, the Hall vector \mathcal{M} behaves like the magnetization vector \mathbf{M} (see Refs. [13, 22, 23] and Supplementary Note 1 for details). This establishes the correspondence between $(\sigma_{zy}, \sigma_{xz}, \sigma_{yx})$ and (M_x, M_y, M_z) .

For a material with magnetic order parameter L , the $\sigma_{\alpha\beta}$ conductivity depends on the orientation of L . To show this, we rewrite $\sigma_{\alpha\beta}$ as $\sigma_{\alpha\beta}(L)$. We recall that time-reversal symmetry links $+L$ with $-L$ magnetic order parameter. The Onsager reciprocity relation further requires that $\sigma_{\alpha\beta}(+L) = \sigma_{\beta\alpha}(-L)$ [5, 22, 23, 33] and this yields

$$\sigma_{\alpha\beta}(+L) = -\sigma_{\alpha\beta}(-L), \quad (2)$$

according to the anti-symmetric feature of $\sigma_{\alpha\beta}$. This indicates that the anomalous Hall conductivity can be reversed by reversing the magnetic order parameter.

Anomalous Hall effect in magnets.— We move on to explore the AHE in crystalline materials. Because of the linkage between AHE and magnetization, we are interested in the magnetization in materials that is spontaneously existing or induced by external stimuli. According to Refs. [25, 34], the existence or absence of magnetization in crystalline materials is determined by their magnetic point groups. For instance, the $m'm2'$ MPG contains 4 symmetry operations, namely, an identity operation ($\mathbf{1}$), a mirror plane perpendicular to x followed by a time-reversal (\mathbf{m}'_x), a mirror plane perpendicular to y (\mathbf{m}_y), and a twofold rotation along z followed by a time-reversal (z'_z). The $\mathbf{1}$, \mathbf{m}'_x , \mathbf{m}_y and z'_z operations transform (M_x, M_y, M_z) to (M_x, M_y, M_z) , $(-M_x, M_y, M_z)$, $(-M_x, M_y, -M_z)$, and $(M_x, M_y, -M_z)$, respectively. This means that M_y is invariant under the 4 symmetry operations, and the $m'm2'$ MPG enables M_y magnetization.

If an MPG is not compatible with M_α magnetization, there must be one or more symmetry operations in this MPG forbidding M_α . An avenue towards M_α is to break such symmetry operations by external fields. Thanks to magnetoelectric coupling [24–26], applying electric field might induce magnetization. To demonstrate this, we again take the $m'm2'$ MPG as an example. In $m'm2'$ MPG, both \mathbf{m}_y and z'_z symmetry operations forbid M_z magnetization, because $\mathbf{m}_y : M_z \rightarrow -M_z$ and $z'_z : M_z \rightarrow -M_z$. Applying a uni-axial electric field E_y naturally breaks \mathbf{m}_y and z'_z symmetries (i.e., $\mathbf{m}_y : E_y \rightarrow -E_y$, $z'_z : E_y \rightarrow -E_y$), which generates an M_z magnetization. By comparison, applying a uni-axial

E_x , E_y , or E_z electric field is insufficient to induce M_x magnetization. As a matter of fact, M_x is forbidden by \mathbf{m}'_x and \mathbf{m}_y , with $\mathbf{m}'_x : (E_x, E_y, E_z) \rightarrow (-E_x, E_y, E_z)$ and $\mathbf{m}_y : (E_x, E_y, E_z) \rightarrow (E_x, -E_y, E_z)$. The E_x electric field preserves \mathbf{m}_y symmetry, E_y preserves \mathbf{m}'_x , and E_z preserves both \mathbf{m}_y and \mathbf{m}'_x . In such sense, the uni-axial E_α (α being x , y , or z) electric field preserves either \mathbf{m}'_x or \mathbf{m}_y symmetry, and this forbids M_x . Applying a bi-axial electric field $[E_x, E_y]$ simultaneously breaks \mathbf{m}'_x and \mathbf{m}_y symmetries, yielding the M_x magnetization.

By similar procedures, we perform symmetry analysis on the entire 122 MPGs, as detailed in Supplementary Note 2. Among these MPGs, 32 type-II MPGs exhibit time-reversal symmetry \hat{T} , which transforms M_α to $-M_\alpha$ ($\alpha = x, y, z$) and forbids the magnetization. Since electric field does not break \hat{T} symmetry, type-II MPGs do not host electric-field induced magnetization. We therefore omit the discussion on type-II MPGs. As for type-I and type-III MPGs, spontaneous and/or electric-field driven magnetization may be allowed by symmetry. Further, the occurrence of M_x , M_y , and M_z implies σ_{zy} , σ_{xz} , and σ_{yx} conductivities, respectively (see the previous section). In Table I, we list the 90 type-I and type-III MPGs with respect to the spontaneous or electric-field driven anomalous Hall conductivity components, where components driven by null, uni-axial, bi-axial, or tri-axial electric field are marked by different color codes.

Phenomenological theory.— In this section, we establish the phenomenological theory for the spontaneous and electric-field driven AHE. We work with the magnetization component M_α , and recall that M_α is rooted in the $B_{\text{eff}}^\alpha M_\alpha$ coupling — B_{eff}^α being an effective magnetic field along α direction. Expanding B_{eff}^α with respect to electric field yields

$$B_{\text{eff}}^\alpha = \lambda_\alpha + \sum_{\beta} \lambda_{\alpha\beta} E_\beta + \sum_{\beta\gamma} \lambda_{\alpha\beta\gamma} E_\beta E_\gamma + \sum_{\beta\gamma\delta} \lambda_{\alpha\beta\gamma\delta} E_\beta E_\gamma E_\delta + \dots, \quad (3)$$

with α , β , γ , and δ labelling the Cartesian direction. The λ_α coefficient in Eq. (3) implies the possible spontaneous M_α magnetization, while $\lambda_{\alpha\beta}$, $\lambda_{\alpha\beta\gamma}$, and $\lambda_{\alpha\beta\gamma\delta}$ characterize the first-order, second-order, and third-order magnetoelectric couplings, respectively.

Essentially, the analytical form of B_{eff}^α is governed by symmetry. In Supplementary Note 2, we derive the B_{eff}^α effective magnetic fields for the 90 type-I and type-III MPGs (see Subsection 2.2 and Supplementary Tables 9, 10, and 11). For several MPGs, the effective magnetic fields B_{eff}^α are not null even in the absence of external electric fields. This is exemplified by the $\bar{1}1$ MPG with $B_{\text{eff}}^x = \lambda_x$, $B_{\text{eff}}^y = \lambda_y$, and $B_{\text{eff}}^z = \lambda_z$ (see Supplementary Table 9). Hence, M_x , M_y , and M_z (i.e., σ_{zy} , σ_{xz} , σ_{yx}) components are enabled in $\bar{1}1$ MPG. In other cases, the

TABLE I. **The anomalous Hall effect in type-I and type-III MPGs.** For each MPG, different color codes are employed to mark the anomalous Hall conductivity components which occur spontaneously or which are driven by electric field. Specifically, the grey rectangles mark the spontaneous components; The single red, cyan, and yellow rectangles indicate the components driven by uni-axial E_x , E_y , and E_z electric fields, respectively; The vertically bipartite rectangles with two colors (among red, cyan, and yellow) represent the components driven by bi-axial $[E_x, E_y]$, $[E_x, E_z]$, or $[E_y, E_z]$ electric field; The vertically tripartite rectangles with red, cyan, and yellow colors denote the components driven by tri-axial $[E_x, E_y, E_z]$ electric field. On the other hand, these conductivity components associated with uni-axial E_β , bi-axial $[E_\beta, E_\gamma]$, and tri-axial $[E_\beta, E_\gamma, E_\delta]$ may respond to $E_\beta^{l_\beta}$, $E_\beta^{m_\beta} E_\gamma^{m_\gamma}$, and $E_\beta^{n_\beta} E_\gamma^{n_\gamma} E_\delta^{n_\delta}$, respectively. In each entry, the orders of electric fields (i.e., l_β , m_β , m_γ , n_β , n_γ , and n_δ) are indicated by numbers, where higher-order responses are omitted. For some cases, the conductivity components might respond to electric fields via different mechanisms but involving identical number of electric field components (e.g., both $[E_x, E_y]$ and $[E_x, E_z]$ involve 2 electric field components). On this condition, different mechanisms towards anomalous Hall conductivity components (separated by space) are shown in the corresponding entries. For instance, the $\bar{6}m2.1$ MPG enables a σ_{yx} component driven by uni-axial E_x (responding to E_x^3), a σ_{xz} driven by $[E_x, E_z]$ bi-axial electric field (responding to $E_x E_z$), and a σ_{zy} driven by bi-axial electric field $[E_x, E_z]$ (responding to $E_x^2 E_z$) or $[E_y, E_z]$ (responding to $E_y E_z$).

MPG	σ_{zy}	σ_{xz}	σ_{yx}	MPG	σ_{zy}	σ_{xz}	σ_{yx}	MPG	σ_{zy}	σ_{xz}	σ_{yx}	MPG	σ_{zy}	σ_{xz}	σ_{yx}				
1.1	Grey	Grey	Grey	$\bar{1}.1$	Grey	Grey	Grey	$\bar{1}'$	1 1 1	1 1 1	1 1 1	2.1	1 1	1 1	Grey				
$2'$	Grey	Grey	1 1	$m.1$	1	1	Grey	m'	Grey	Grey	1	$2/m.1$	1 1	1 1	Grey				
$2'/m$	1	1	1 1	$2/m'$	1 1	1 1	1	$2'/m'$	Grey	Grey	1 1	222.1	1	1	1				
$2'2'2$	1	1	Grey	$mm2.1$	1	1	1 1	$m'm'2'$	1 1	Grey	1	$m'm'2$	1	1	Grey				
$mmm.1$	1 1	1 1	1 1	$m'mm$	1 1	1	1	$m'm'm$	1 1	1 1	Grey	$m'm'm'$	1	1	1				
4.1	1 1	1 1	Grey	$4'$	1 1	1 1	2 2	$\bar{4}.1$	1 1	1 1	Grey	$\bar{4}'$	1 1	1 1	2 2 1				
$4/m.1$	1 1	1 1	Grey	$4'/m$	1 1	1 1	2 2	$4/m'$	1 1	1 1	1	$4'/m'$	1 1	1 1	1 2				
422.1	1	1	1	$4'22'$	1	1	1 1 1	$42'2'$	1	1	Grey	$4mm.1$	1	1	3 1				
$4'm'm$	1	1	2 2	$4m'm'$	1	1	Grey	$\bar{4}2m.1$	1	1	3 1 1	$\bar{4}'2'm$	1	1	2 2				
$\bar{4}'2m'$	1	1	1	$\bar{4}2'm'$	1	1	Grey	$4/mmm.1$	1 1	1 1	3 1	$4/m'mm$	1	1	1 1 1				
$4'/mm'm$	1 1	1 1	2 2	$4'/m'm'm$	1	1	1 1 1	$4/mm'm'$	1 1	1 1	Grey	$4/m'm'm'$	1	1	1				
3.1	1 1	1 1	Grey	$\bar{3}.1$	2 2	2 2	Grey	$\bar{3}'$	1 1	1 1	3 3 1	32.1	1 2	1	3 1				
$32'$	1	1 2	Grey	$3m.1$	2 1	1	3	$3m'$	1	2 1	Grey	$\bar{3}m.1$	2 2	1 1	3 1 1				
$\bar{3}'m$	1	1	3	$\bar{3}'m'$	1	1	3 1	$\bar{3}m'$	1 1	2 2	Grey	6.1	1 1	1 1	Grey				
$6'$	2 2	2 2	3 3	$\bar{6}.1$	1 1	1 1	Grey	$\bar{6}'$	1 1	1 1	1	$6/m.1$	1 1	1 1	Grey				
$6'/m$	1 1	1 1	3 3	$6/m'$	1 1	1 1	1	$6'/m'$	2 2	2 2	1 1	622.1	1	1	1				
$6'22'$	2 2	1 1 1	3	$62'2'$	1	1	Grey	$6mm.1$	1	1	3 3	$6'mm'$	2 2	1 1	3				
$\bar{6}m'm'$	1	1	Grey	$\bar{6}m2.1$	1 1	1 1	3	$\bar{6}'m'2$	1	2 1	1	$\bar{6}'m'2'$	2 1	1	1 3				
$\bar{6}m'2'$	1 1	1 1	Grey	$6/mmm.1$	1 1	1 1	3 3	$6/m'mm$	1	1	1 3	$6'/mmm'$	1 1	1 1	3 1				
$6'/m'mm'$	2 2	1 1	3	$6/m'm'm'$	1 1	1 1	Grey	$6/m'm'm'$	1	1	1	23.1	1	1	1				
$m\bar{3}.1$	1 1	1 1	1 1	$m'\bar{3}'$	1	1	1	432.1	1	1	1	$4'32'$	2 1 1	1 2 1	1 1 1				
$\bar{4}3m.1$	2 3 2	1 2 3	3 1 1	$\bar{4}'3m'$	1	1	1	$m\bar{3}m.1$	3 1	3 1	3 1	$m'\bar{3}'m$	2 2	1 2	1 1 1				
$m\bar{3}m'$	1 1	1 1	1 1	$m'\bar{3}'m'$	1	1	1	Spontaneous: Grey			E_x : Red			E_y : Cyan			E_z : Yellow		

B_{eff}^α fields are driven by external electric field. As shown in Supplementary Table 10, the effective magnetic fields

associated with $\bar{6}m2.1$ MPG are given by

$$\begin{aligned}
B_{\text{eff}}^x &= \lambda_{xxxz}(E_x^2 - E_y^2)E_z + \lambda_{xyz}E_yE_z, \\
B_{\text{eff}}^y &= -2\lambda_{xxxz}E_xE_yE_z - \lambda_{xyz}E_xE_z, \\
B_{\text{eff}}^z &= \lambda_{zzxx}E_x(E_x^2 - 3E_y^2).
\end{aligned} \tag{4}$$

The B_{eff}^x field is a function of E_x , E_y , and E_z , where (i) $\lambda_{xxxz}E_x^2E_z$ implies the third-order magnetoelectric coupling created by $[E_x, E_z]$ bi-axial electric field, (ii) $\lambda_{xyz}E_yE_z$ implies the second-order magnetoelectric coupling due to $[E_y, E_z]$, and (iii) $\lambda_{xxxz}E_y^2E_z$ implies third-order magnetoelectric coupling driven by $[E_y, E_z]$. Associated with $[E_y, E_z]$, both $\lambda_{xyz}E_yE_z$ and $\lambda_{xxxz}E_y^2E_z$ are valid, and the former is the primary contribution for M_x . As for $[E_x, E_z]$, the lowest-order contribution is $\lambda_{xxxz}E_x^2E_z$. In such sense, Eq. (4) indicates that M_x and σ_{zy} can be *primarily* driven by $[E_x, E_z]$ via $\lambda_{xxxz}E_x^2E_z$, or $[E_y, E_z]$ via $\lambda_{xyz}E_yE_z$ ($E_y^2E_z$ being a secondary contribution). Similarly, B_{eff}^y is induced by either bi-axial $[E_x, E_z]$ or tri-axial $[E_x, E_y, E_z]$ electric field. On this condition, we are only interested in the M_y and σ_{xz} driven by bi-axial $[E_x, E_z]$ electric field, since the orientation of the tri-axial electric field is more complex compared to the bi-axial case. The B_{eff}^z effective magnetic field is driven by uni-axial E_x or bi-axial $[E_x, E_y]$ electric field — the former being the case we are interested in. In short, the $\bar{6}m2.1$ MPG enables σ_{zy} , σ_{xz} , and σ_{yx} , where σ_{zy} responds to $E_x^2E_z$ or E_yE_z , σ_{xz} responds to E_xE_z , and σ_{yx} responds to E_x^3 (see Table I). Following similar conventions, we analyze the effective magnetic fields for the other type-I and type-III MPGs, and summarize the results in Table I.

Before finishing this section, it is important to discuss several special cases regarding Table I. An example is given by the $4mm.1$ MPG (see Supplementary Table 9), for which $B_{\text{eff}}^z = \lambda_{zxxx}E_xE_y(E_x^2 - E_y^2)$. As a matter of fact, the σ_{yx} conductivity is induced by bi-axial $[E_x, E_y]$ electric field, via fourth-order magnetoelectric coupling $E_x^3E_y$ or $E_xE_y^3$. To save ink in Table I, we only show the $E_x^3E_y$ case but omit $E_xE_y^3$. Note, however, that $E_x^3E_y$ and $E_xE_y^3$ have equal rights toward σ_{yx} . When $|E_x| = |E_y|$, $B_{\text{eff}}^z = \lambda_{zxxx}E_xE_y(E_x^2 - E_y^2)$ becomes zero and this yields null σ_{yx} conductivity (σ_{yx} being quenched) in the regime of fourth-order magnetoelectric coupling. Such a quenching behavior appears in 10 MPGs on the condition that bi-axial or tri-axial electric field is along specific directions, summarized in Supplementary Table 12.

Electric-field driven AHE in Cr_2O_3 and CoF_2 .— We now explore semiconductors that exhibit electric-field driven AHE. As shown in Table I, a vast majority of MPGs enable such a feature and materials belonging to these MPGs can be identified thanks to the MAGNDATA database [35, 36]. From the database, we select Cr_2O_3 and CoF_2 as two representative materials. These two materials have no more than 10 ions per primitive cell, for which the computational costs are affordable.

Cr_2O_3 has a Néel temperature of 307 K and belongs to the $\bar{3}'m'$ MPG [37, 38]. The crystal and magnetic structures of Cr_2O_3 are sketched in Fig. 1(a). According to Table I, Cr_2O_3 with $+L$ magnetic order pa-

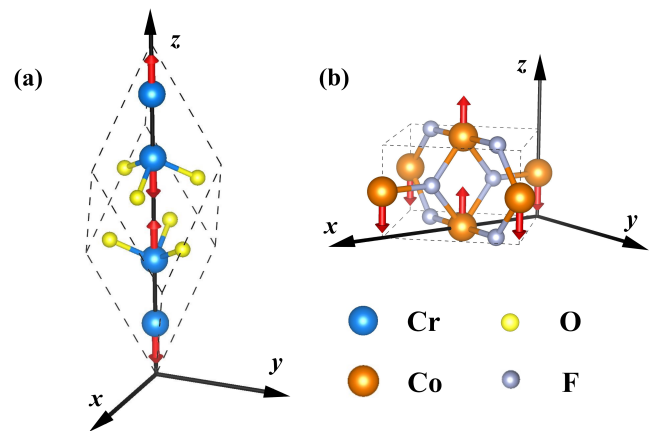


FIG. 1. **The crystal and magnetic structures for two compounds.** The Cr, Co, O and F ions are denoted by cyan, orange, yellow and grey spheres, respectively. The magnetic moments are shown by red arrows. (a): Cr_2O_3 with $+L$ magnetic order parameter. (b): CoF_2 with $+L$ magnetic order parameter. The x , y , and z directions in both panels are orthogonal to each other.

rameter enables (i) σ_{zy} conductivity driven by E_x , (ii) σ_{xz} conductivity driven by E_y , and (iii) σ_{yx} conductivity driven by E_z or E_y^3 . Furthermore, switching the magnetic order parameter from $+L$ to $-L$ reverses the aforementioned electric-field induced Hall conductivity, namely, $\sigma_{\alpha\beta}(+L) = -\sigma_{\alpha\beta}(-L)$ [see Eq. (2)]. This is verified by various anomalous Hall conductivity components of Cr_2O_3 computed by first-principles, as shown in Figs. 2(a)-(d). To be specific, σ_{zy} , σ_{xz} , and σ_{yx} components remain zero in the absence of an external electric field; Such components are driven by E_x , E_y , or E_z electric field, where the induced conductivities associated with $+L$ and $-L$ are basically opposite by sign. As shown in Figs. 2(a), (b) and (d), σ_{zy} , σ_{xz} , and σ_{yx} can be larger than 100 S/cm. These conductivities are driven by E_x , E_y , or E_z electric field (magnitude being 4 MV/cm) via first-order response. Instead, the maximum value of σ_{yx} , driven by $E_y = 4$ MV/cm via third-order response, is less than 20 S/cm [see Fig. 2(c)]. Interestingly, Figs. 2(a) and (b) are quite similar, and this is understandable by examining the effective magnetic fields associated with $\bar{3}'m'$ MPG. In Supplementary Table 10, we find that $B_{\text{eff}}^x = \lambda_{xx}E_x$ and $B_{\text{eff}}^y = \lambda_{xx}E_y$ for $\bar{3}'m'$ MPG, where the shared λ_{xx} coefficient implies that σ_{zy} and σ_{xz} are symmetrically related.

Another interesting material is CoF_2 which has a Néel temperature of 39 K [39–41]. In Fig. 1(b), we schematically show the crystal and magnetic structures for CoF_2 . Under such a coordinate system, the MPG of CoF_2 is $4'/mm'm$ — being the MPG for the $P4'/mmm'$ magnetic space group [42, 43]. As shown in Table I, unlike Cr_2O_3 , the anomalous Hall conductivities in CoF_2 respond to electric field via second order. Specifically,

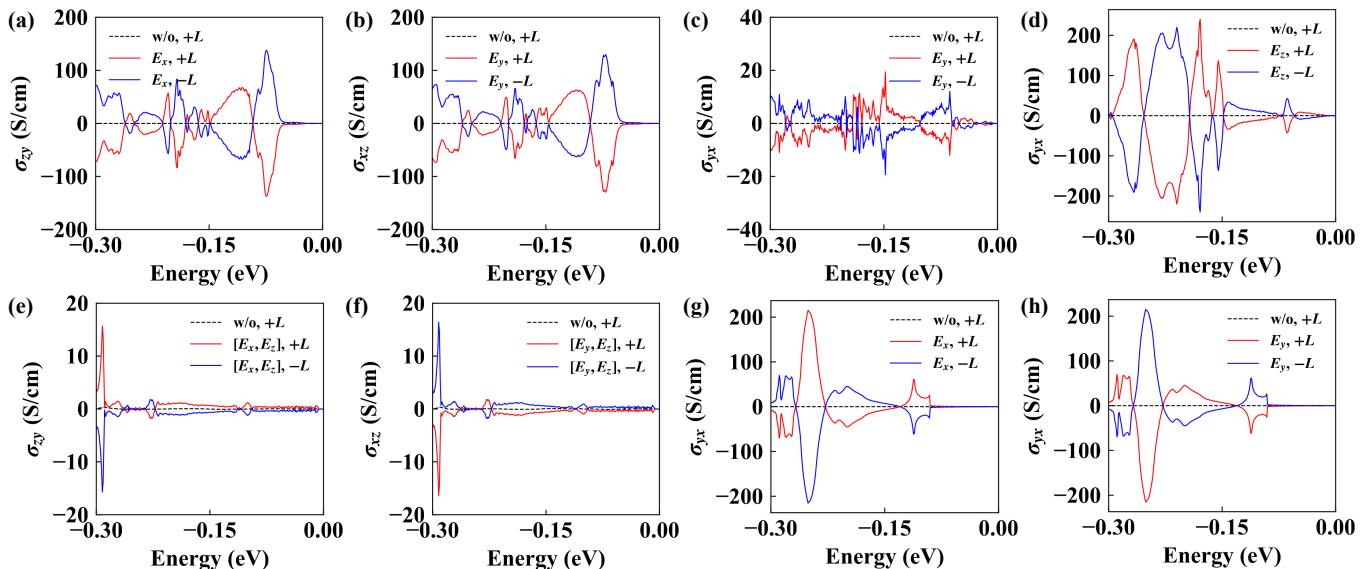


FIG. 2. The electric-field driven anomalous Hall conductivities in Cr_2O_3 and CoF_2 as a function of chemical potential (defined with respect to the Fermi level). Panels (a)-(d) depict the anomalous Hall conductivity in Cr_2O_3 , with σ_{xy} , σ_{xz} , σ_{yx} , and σ_{yx} being driven by E_x , E_y , E_y , and E_z , respectively. Panels (e)-(h) show the anomalous Hall conductivity in CoF_2 , with σ_{zy} , σ_{xz} , σ_{xy} , and σ_{xy} being driven by $[E_x, E_z]$, $[E_y, E_z]$, E_x , E_y , respectively.

σ_{yx} is driven by uni-axial E_x^2 or E_y^2 response, while σ_{zy} and σ_{xz} are from bi-axial $E_x E_z$ and $E_y E_z$ responses, respectively. Our first-principles calculations illustrated in Figs. 2(e)-(h), corroborate our aforementioned analysis and further confirm that reversing the magnetic order parameter (in CoF_2) reverses the anomalous Hall conductivities. For $E_x = E_z = 2\sqrt{2}$ MV/cm and $E_y = E_z = 2\sqrt{2}$ MV/cm (i.e., the total amplitude being 4 MV/cm), σ_{zy} and σ_{xz} can reach 10 S/cm, whereas an electric field of $E_x = 4$ MV/cm or $E_y = 4$ MV/cm can yield σ_{yx} being larger than 200 S/cm. Moreover, the resemblance between Figs. 2(e) and (f) [respectively, Figs. 2(g) and (h)] is reflected in the effective magnetic fields associated with $4'/mm'm$ MPG: $B_{\text{eff}}^x = \lambda_{xxz} E_x E_z$ and $B_{\text{eff}}^y = -\lambda_{xxz} E_y E_z$ [respectively, $B_{\text{eff}}^z = \lambda_{zxx} (E_x^2 - E_y^2)$] (see Supplementary Table 9).

Summary and outlook.— In the present work, we establish the phenomenological theory for the anomalous Hall effect in magnets. By symmetry analysis, we show that the anomalous Hall conductivities in magnets can either spontaneously appear or be driven by electric fields via linear or nonlinear magnetoelectric coupling. Such anomalous Hall conductivities are governed by magnetic point group symmetries and are hosted by 90 type-I and type-III magnetic point groups (summarized in Table I). To testify our theory, we further propose Cr_2O_3 and CoF_2 (by first-principles calculations) as candidate materials showcasing electric-field induced anomalous Hall conductivities. Strikingly, the $+L$ and $-L$ magnetic order parameters in magnets yield spontaneous or

electric-field induced anomalous Hall conductivities with opposite signs. As such, we hope that our work will enrich the means for detecting the magnetic order parameters in magnets, which is of practical importance for spintronics [31, 44–51].

Acknowledgements.— The authors acknowledge the support from National Natural Science Foundation of China (Grants No. 12274174, No. 12274102, No. 22090044, No. 52288102, No. 52090024, and No. 12034009), the Strategic 373 Priority Research Program of Chinese Academy of Sciences (Grant No. XDB33000000). L.B. acknowledges support from the Vannevar Bush Faculty Fellowship (VBFF) from the Department of Defense and Award No. DMR-1906383 from the National Science Foundation Q-AMASE-i Program (MonArk NSF Quantum Foundry). L.J.Y. thanks the support from the high-performance computing center of Jilin University. H.J.Z. thanks the “Xiaomi Young Scholar” Project.

-
- [1] D. Xiao, M.-C. Chang, and Q. Niu, *Rev. Mod. Phys.* **82**, 1959 (2010).
 - [2] T. Jungwirth, Q. Niu, and A. H. MacDonald, *Phys. Rev. Lett.* **88**, 207208 (2002).
 - [3] M. Onoda and N. Nagaosa, *J. Phys. Soc. Jpn* **71**, 19 (2002).
 - [4] L. Bellaïche, W. Ren, and S. Singh, *Phys. Rev. B* **88**, 161102 (2013).
 - [5] N. Nagaosa, J. Sinova, S. Onoda, A. H. MacDonald, and

- N. P. Ong, *Rev. Mod. Phys.* **82**, 1539 (2010).
- [6] R. Karplus and J. Luttinger, *Phys. Rev.* **95**, 1154 (1954).
- [7] J. Smit, *Physica* **21**, 877 (1955).
- [8] J. Smit, *Physica* **24**, 39 (1958).
- [9] L. Berger, *Phys. Rev. B* **2**, 4559 (1970).
- [10] R. G. Betancourt, J. Zubáć, R. Gonzalez-Hernandez, K. Geishendorf, Z. Šobáň, G. Springholz, K. Olejník, L. Šmejkal, J. Sinova, T. Jungwirth, *et al.*, *Phys. Rev. Lett.* **130**, 036702 (2023).
- [11] A. K. Nayak, J. E. Fischer, Y. Sun, B. Yan, J. Karel, A. C. Komarek, C. Shekhar, N. Kumar, W. Schnelle, J. Kübler, *et al.*, *Sci. Adv.* **2**, e1501870 (2016).
- [12] S. Nakatsuji, N. Kiyohara, and T. Higo, *Nature* **527**, 212 (2015).
- [13] L. Šmejkal, R. González-Hernández, T. Jungwirth, and J. Sinova, *Sci. Adv.* **6**, eaaz8809 (2020).
- [14] X. Li, J. Koo, Z. Zhu, K. Behnia, and B. Yan, *Nat. Commun.* **14**, 1642 (2023).
- [15] L. Šmejkal, A. H. MacDonald, J. Sinova, S. Nakatsuji, and T. Jungwirth, *Nat. Rev. Mater.* **7**, 482 (2022).
- [16] H. Reichlova, R. Lopes Seeger, R. González-Hernández, I. Kounta, R. Schlitz, D. Kriegner, P. Ritzinger, M. Lamme, M. Leiviskä, A. Birk Hellenes, *et al.*, *Nat. Commun.* **15**, 4961 (2024).
- [17] M. Wang, K. Tanaka, S. Sakai, Z. Wang, K. Deng, Y. Lyu, C. Li, D. Tian, S. Shen, N. Ogawa, *et al.*, *Nat. Commun.* **14**, 8240 (2023).
- [18] M. Ikhlas, S. Dasgupta, F. Theuss, T. Higo, S. Kittaka, B. Ramshaw, O. Tchernyshyov, C. Hicks, and S. Nakatsuji, *Nat. Phys.* **18**, 1086 (2022).
- [19] L. Han, X. Fu, R. Peng, X. Cheng, J. Dai, L. Liu, Y. Li, Y. Zhang, W. Zhu, H. Bai, *et al.*, *Sci. Adv.* **10**, eadn0479 (2024).
- [20] Z. Feng, X. Zhou, L. Šmejkal, L. Wu, Z. Zhu, H. Guo, R. González-Hernández, X. Wang, H. Yan, P. Qin, *et al.*, *Nat. Electron.* **5**, 735 (2022).
- [21] R. Gonzalez Betancourt, J. Zubáć, R. Gonzalez-Hernandez, K. Geishendorf, Z. Šobáň, G. Springholz, K. Olejník, L. Šmejkal, J. Sinova, T. Jungwirth, *et al.*, *Phys. Rev. Lett.* **130**, 036702 (2023).
- [22] H. Grimmer, *Acta Crystallogr. A* **49**, 763 (1993).
- [23] M. Seemann, D. Ködderitzsch, S. Wimmer, and H. Ebert, *Phys. Rev. B* **92**, 155138 (2015).
- [24] M. Fiebig, *J. Phys. D: Appl. Phys.* **38**, R123 (2005).
- [25] H. Schmid, *Int. J. Magn* **4**, 2 (1973).
- [26] H. Schmid, *Ferroelectrics* **161**, 1 (1994).
- [27] W.-B. Dai, H. Li, D.-H. Xu, C.-Z. Chen, and X. C. Xie, *Phys. Rev. B* **106**, 245425 (2022).
- [28] R. Chen, H.-P. Sun, M. Gu, C.-B. Hua, Q. Liu, H.-Z. Lu, and X. Xie, *Natl. Sci. Rev.* **11**, nwac140 (2024).
- [29] A. Gao, Y.-F. Liu, C. Hu, J.-X. Qiu, C. Tzschaschel, B. Ghosh, S.-C. Ho, D. Bérubé, R. Chen, H. Sun, *et al.*, *Nature* **595**, 521 (2021).
- [30] C. Cui, R.-W. Zhang, Y. Han, Z.-M. Yu, and Y. Yao, Electric hall effect and quantum electric hall effect (2024), arXiv:2405.15410 [cond-mat.mes-hall].
- [31] L. L. Tao, Q. Zhang, H. Li, H. J. Zhao, X. Wang, B. Song, E. Y. Tsymbal, and L. Bellaiche, *Phys. Rev. Lett.* **133**, 096803 (2024).
- [32] MPGs are categorized into three types, namely (i) type-I MPGs involving only spatial operations and lacking time-reversal operation; (ii) type-II MPGs incorporating time-reversal as an independent operation; and (iii) type-III MPGs containing time-reversal operation only in combination with spatial operations. More details are provided in Ref. [34].
- [33] S. Shtrikman and H. Thomas, *Solid State Commun.* **3**, 147 (1965).
- [34] M. S. Dresselhaus, G. Dresselhaus, and A. Jorio, *Group theory: application to the physics of condensed matter* (Springer Science & Business Media, 2007).
- [35] S. V. Gallego, J. M. Perez-Mato, L. Elcoro, E. S. Tasci, R. M. Hanson, K. Momma, M. I. Aroyo, and G. Madariaga, *J. Appl. Crystallogr.* **49**, 1750 (2016).
- [36] S. V. Gallego, J. M. Perez-Mato, L. Elcoro, E. S. Tasci, R. M. Hanson, M. I. Aroyo, and G. Madariaga, *J. Appl. Crystallogr.* **49**, 1941 (2016).
- [37] P. Brown, J. Forsyth, E. Lelièvre-Berna, and F. Tasset, *J. Phys.: Condens. Matter* **14**, 1957 (2002).
- [38] A. Mahmood, W. Echtenkamp, M. Street, J.-L. Wang, S. Cao, T. Komesu, P. A. Dowben, P. Buragohain, H. Lu, A. Gruverman, *et al.*, *Nat. Commun.* **12**, 1674 (2021).
- [39] R. Thomson, T. Chatterji, and M. Carpenter, *J. Phys.: Condens. Matter* **26**, 146001 (2014).
- [40] T. W. Metzger, K. A. Grishunin, C. Reinhofer, R. M. Dubrovin, A. Arshad, I. Ilyakov, T. V. de Oliveira, A. Ponomaryov, J.-C. Deinert, S. Kovalev, *et al.*, *Nat. Commun.* **15**, 5472 (2024).
- [41] E. A. Mashkovich, K. A. Grishunin, R. M. Dubrovin, A. K. Zvezdin, R. V. Pisarev, and A. V. Kimel, *Science* **374**, 1608 (2021).
- [42] W. Jauch, M. Reehuis, and A. Schultz, *Acta Crystallogr. A* **60**, 51 (2004).
- [43] R. M. Dubrovin, A. Tellez-Mora, A. C. Garcia-Castro, N. V. Siverin, N. N. Novikova, K. N. Boldyrev, E. A. Mashkovich, A. H. Romero, and R. V. Pisarev, *Phys. Rev. B* **109**, 224312 (2024).
- [44] T. Jungwirth, J. Sinova, A. Manchon, X. Marti, J. Wunderlich, and C. Felser, *Nat. Phys.* **14**, 200 (2018).
- [45] V. Baltz, A. Manchon, M. Tsoi, T. Moriyama, T. Ono, and Y. Tserkovnyak, *Rev. Mod. Phys.* **90**, 015005 (2018).
- [46] P. Němec, M. Fiebig, T. Kampfrath, and A. V. Kimel, *Nat. Phys.* **14**, 229 (2018).
- [47] J. Han, R. Cheng, L. Liu, H. Ohno, and S. Fukami, *Nat. Mater.* **22**, 684 (2023).
- [48] D.-F. Shao, S.-H. Zhang, G. Gurung, W. Yang, and E. Y. Tsymbal, *Phys. Rev. Lett.* **124**, 067203 (2020).
- [49] J. Wang, H. Zeng, W. Duan, and H. Huang, *Phys. Rev. Lett.* **131**, 056401 (2023).
- [50] P. Wadley, B. Howells, J. Železný, C. Andrews, V. Hills, R. P. Campion, V. Novák, K. Olejník, F. Maccherozzi, S. Dhesi, *et al.*, *Science* **351**, 587 (2016).
- [51] J. Železný, P. Wadley, K. Olejník, A. Hoffmann, and H. Ohno, *Nat. Phys.* **14**, 220 (2018).